Journal of the European Ceramic Society 20 (2000) 1003–1010

Dielectric and pyroelectric properties of Nb-doped $Pb(Zr_{0.92}Ti_{0.08})O_3$ ceramics

Z. Ujma [a,*], L. Szymczak [a], J. Hańderek [a], K. Szot [a], H.J. Penkalla [b]

[a] *Institute of Physics, University of Silesia, Uniwersytecka 4, 40-007 Katowice, Poland*
[b] *Institut für Werkstoffe und Verfahren der Energietechnik, Forschungszentrum Jülich, D-52425 Jülich, Germany*

Received 22 April 1999; received in revised form 29 July 1999; accepted 8 August 1999

Abstract

Dielectric and pyroelectric characteristics and changes of electric conductivity were investigated for Nb_2O_5-doped $Pb(Zr_{0.92}Ti_{0.08})O_3$ ceramics. The influence of this dopant on the ceramics microstructure was also studied. Correlation between the investigated electric characteristics and grain structure was confirmed. Some progress in understanding the influence of Nb-dopant was reached in this way.

Keywords: Dielectric properties; Electrical conductivity; Pyroelectric properties; PZT

1. Introduction

It is well known that useful characteristics and parameters of $Pb(Zr_{1-x},Ti_x)O_3$ ceramics (PZT) can be obtained by suitable selection of Zr/Ti ratio and by substitution of a small amount of isovalent or heterovalent elements for the Pb or Zr/Ti sublattices.[1–3] So far a number of papers have dealt with the Zr-rich PZT-type ceramics, showing orthorhombic antiferroelectric (A_O) — low temperature rhombohedral ferroelectric ($F_{R(LT)}$) — high temperature rhombohedral ferroelectric ($F_{R(HT)}$) — cubic paraelectric (P_C) phase sequence.[4–13] These ceramics, with Ti contents up to $x = 0.15$, exhibit useful dielectric and pyroelectric characteristics, suitable for pyroelectric detectors, energy converters, imaging systems, etc. In recent years the interest in studies of the Zr-rich PZT-type ceramics has increased again owing to these characteristics and to the emerging possibilities of application.[12,14,15] Some of our recent papers also centred on this kind of PZT and PLZT ceramics, and in particular on those with Zr/Ti ratio from vicinity of 95/5[16,17] and 92/8.[18,19]

As mentioned above, the useful properties of the PZT-type ceramics, including the Zr-rich materials, can be substantially improved by the substitution of selected elements for the Pb or Zr/Ti sublattices. The La and Nb additives are most often used for this purpose. An abundant literature on the subject indicates that these dopants influence temperatures of the structural phase transitions between the phases of various types of the electric order (FE, AFE and PE) and also dielectric, pyroelectric, piezoelectric, electro-optic and other parameters. This in particular concerns the Nb doped Zr-rich $Pb(Zr,Ti)O_3$ ceramics[4,6,7,11–13,17] and also $PbZrO_3$.[20,21] It was shown that the Nb_2O_5 dopant concentration smaller than about 1 mol% is the most favourable, from the properties and applications point of view, whereas its higher content leads to deterioration of these properties. This effect was observed by many authors but its full elucidation has not as yet been achieved.

To reach some progress in the understanding of the influence of Nb_2O_5 added in the amount $0.2 \div 1.5$ mol% to the base composition $Pb(Zr_{0.92}Ti_{0.08})O_3$ we have focused on investigations of the ceramics microstructure, dielectric and pyroelectric properties.

Changes of electric conductivity and Seebeck's coefficient, caused by Nb-additives, were also investigated and discussed.

* Corresponding author. Tel.: +48-32-588211 ext 1134; fax: +48-32-588-431.
E-mail address: ujma@us.edu.pl (Z. Ujma).

0955-2219/00/$ - see front matter
PII: S0955-2219(99)00211-3

2. Ceramics preparation and their grain structure

The $Pb(Zr_{0.92}Ti_{0.08})O_3$ ceramics with Nb_2O_5 content 0.2÷1.5 mol% were prepared using the conventional mixed-oxide processing technique. Stoichiometric amounts of PbO, ZrO_2 and TiO_2 oxides, together with the target amount of Nb_2O_5 additive were weighed and mixed. Thermal synthesis of the pressed mixture was carried out at 950°C for 3 h. Then the crushed, milled and sieved materials were pressed again into cylindrical pellets and sintered at 1100°C for 3 h. Each pellet was placed inside a double crucible with some amount of PbO and ZrO_2 oxides in order to preserve the predetermined composition, and to reduce PbO loss caused by its sublimation. The latter procedure was repeated before the final sintering, carried out at 1260°C for 12 h. The furnace was then cooled to room temperature over a period of 12 h. The obtained ceramics, with 94–96% theoretical density and less than 1% weight loss, were semitransparent and of good mechanical quality.

The grain structure and distribution of all the elements throughout the grains was examined by a scanning electron microscope (SEM), JSM-5410 with an energy dispersive X-ray spectrometer (EDS). The grain size measurements were performed on fracture surface of the ceramics. The images of microstructure of the PZT-92/8 ceramics with Nb_2O_5 content 0.2 and 1.2 mol% are shown in Fig. 1, as an example. The grain sizes were 10–15 μm and 5–10 μm for the ceramics with 0.2 and 1.2 mol% of Nb_2O_5, respectively. The Nb_2O_5 addition produces slightly smaller grains with increasing concentration. In the Nb_2O_5 rich ($\geqslant 1$ mol%) ceramics the "nests" of very small (<1 μm) grains can be seen (Fig. 1(b)). Their quantity was larger in the case of a higher concentration of Nb_2O_5.

The EDS analysis indicated a homogeneous distribution of all the native elements of the ceramics within the larger grains. The TEM-EDX measurement technique was used to find differences in the composition of two kinds of grains, shown in Fig. 1(b). The TEM-microscope (Philips CM200, 200 kV and LaB_6 cathode) was used for these measurements. They were carried out for the mechanically crumbled ceramic samples. The separated grains were sedimented onto the copper preparation grid of the microscope. The EDX analysis of the larger and smaller grains from the ceramics with 1.2 mol% of Nb_2O_5, shown in Fig. 1(b), revealed a difference in their chemical composition. The fragments of EDX spectrum for both larger and smaller grains are shown in Fig. 2(a) and (b), respectively. It can be seen that the smaller grains contain more Nb and considerably less Zr in comparison with the larger grains. Similar measurements, of the ceramics with 0.2 mol% of Nb_2O_5, revealed an identical distribution of Nb and Zr in grains of a different size.

3. Dielectric measurements

The cut and polished 0.6 mm thick samples, coated with silver electrodes, were used for the measurements of dielectric constant and loss tangent as a function of temperature. An automatic measuring system was used to measure and record numerically ε and tan δ at several frequencies of the measuring electric field. Exemplary $\varepsilon(T)$ and tan $\delta(T)$ characteristics, obtained at the measuring field of frequency 1 kHz, for the PZT-92/8 ceramic modified by 0.2 mol% of Nb_2O_5, are shown in Fig. 3. Both $\varepsilon(T)$ and tan $\delta(T)$ curves reveal various anomalies in the vicinities of temperatures corresponding to A_O–$F_{R(LT)}$; $F_{R(LT)}$–$F_{R(HT)}$ and $F_{R(HT)}$–P_C phase transition. They are relatively insignificant in case of the phase transition between two ferroelectric phases and peculiarly distinct at Curie temperature. The comparison of $\varepsilon(T)$ curves, obtained for the ceramics of the base composition $Pb(Zr_{0.92}Ti_{0.08})O_3$ modified by a various amount of Nb_2O_5 additive is shown in Fig. 4(a) and (b) for the temperature ranges containing low and high temperature phase transitions, respectively. One can see that the values of ε in the vicinities of low-temperature

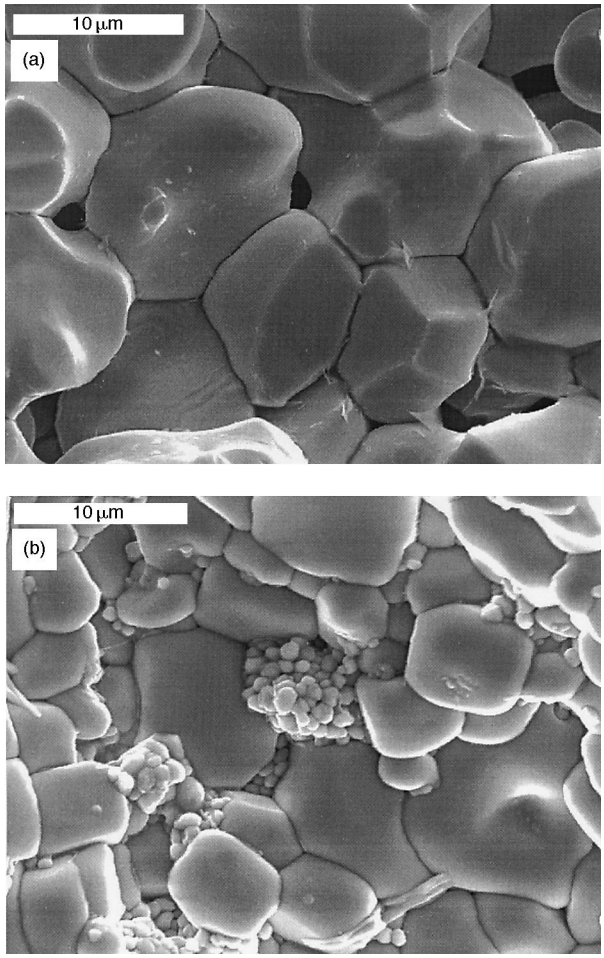

Fig. 1. SEM images of the fracture surface of PZT 92/8 + 0.2 mol% Nb_2O_5 (a) and PZT 92/8 + 1.2 mol% Nb_2O_5 (b) ceramics.

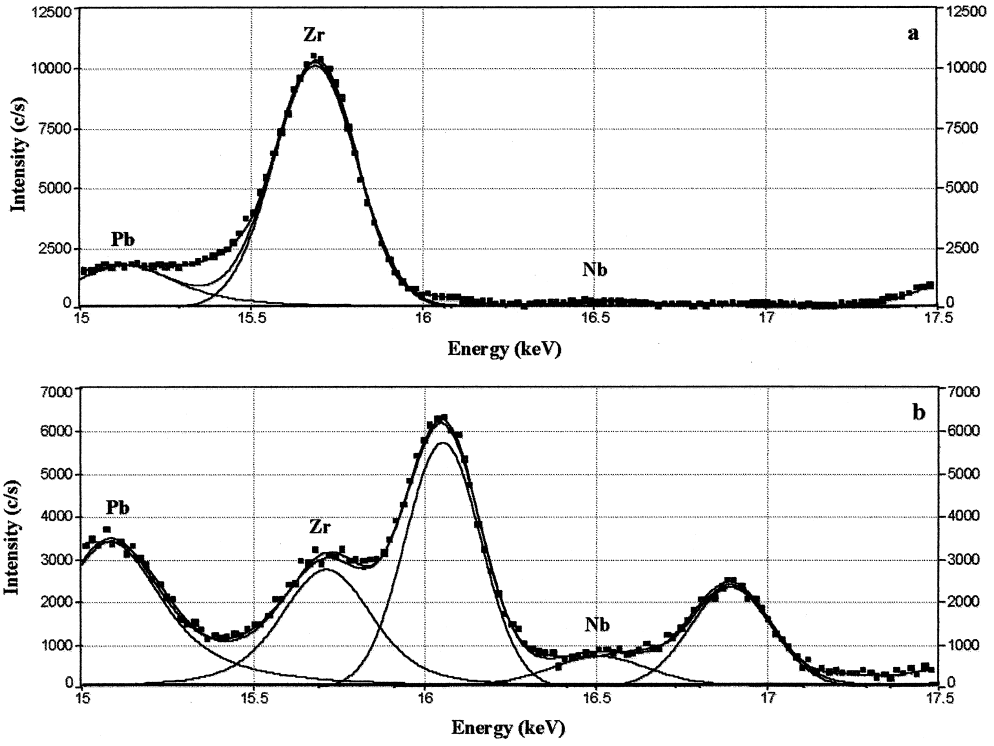

Fig. 2. The EDX analysis of the larger (a) and smaller (b) grains from PZT 92/8 + 1.2 mol% Nb_2O_5 ceramics.

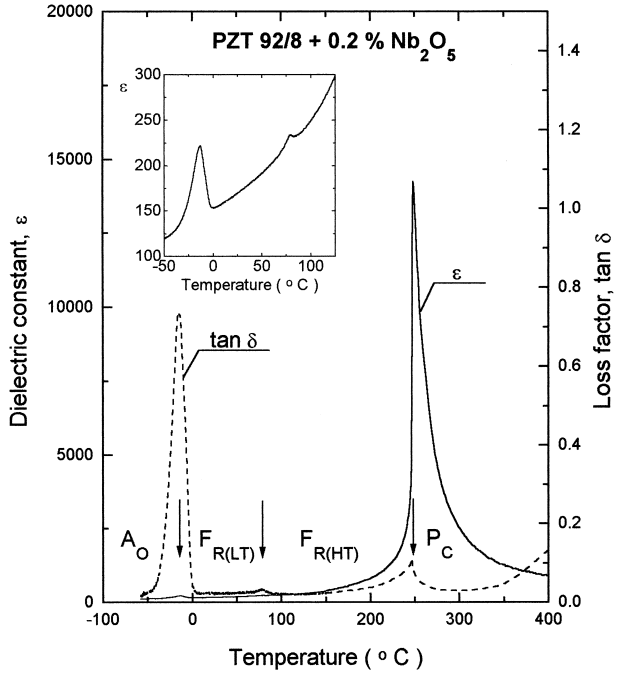

Fig. 3. Dielectric constant and loss factor as a function of temperature, measured on heating at frequency 1 kHz for PZT 92/8 + 0.2 mol% Nb_2O_5 ceramics. The ε vs temperature in the vicinities of the $A_O \rightarrow F_{R(LT)}$ and $F_{R(LT)} \rightarrow F_{R(HT)}$ phase transitions is shown in the inserted figure.

phase transitions rise with the increase in Nb_2O_5 content (Fig. 4(a)). The position of anomalies in the $\varepsilon(T)$ curves, corresponding to the A_O–$F_{R(LT)}$ and $F_{R(LT)}$–$F_{R(HT)}$ phase transitions, is weakly dependent on the Nb content, despite a noticeable increase of the $F_{R(LT)}$–$F_{R(HT)}$ phase transition temperatures (Fig. 5). A linear decrease of the $F_{R(HT)}$–P_C phase transition temperature takes place with an increase of Nb content (Fig. 5). The (values first rise notably and then less rapidly with increase in Nb content (Fig. 4(b)). The maxima in $\varepsilon(T)$ curves become strongly broadened and the values of ε decrease abruptly when the Nb_2O_5 content exceeds 1 mol%.

The examples of $\varepsilon(T)$ curves, obtained at various frequencies of the measuring field, are shown in Fig. 6 for the ceramics with various Nb_2O_5 content. The $\varepsilon(T)$ characteristics are weakly frequency dependent in case of the low Nb content. The same holds for the ceramics with a larger content of Nb_2O_5 in the temperature range $T < \sim 275°C$. In this case an additional, peculiarly broadened, maxima in the $\varepsilon(T)$ curves occurs in the range of higher temperatures, that is in the range of PE phase.

Remanent polarization (P_r) was determined as a function of temperature from the hysteresis loop measurements. Hysteresis loops at 50 Hz and strength 10 kV/cm were examined using the modified Sawyer–Tower method. The temperature dependence of P_r and coercive field (E_c) obtained for the $Pb(Zr_{0.92}Ti_{0.08})O_3$ ceramics with various Nb_2O_5 content, is shown in Fig. 7. The course of the $P_r(T)$ curves differs markedly for the ceramics with Nb_2O_5 content < 1 mol% from that with > 1 mol%. All the investigated ceramics show a remanent polarization of 16–22 $\mu C/cm^2$. In case of ceramics with Nb_2O_5 content of 0.6–1 mol% the P_r value is somewhat larger. The P_r rises slowly on heating

above the A_O–$F_{R(LT)}$ phase transition. The ceramics with the smallest amount of Nb_2O_5 show local minima in the vicinity of the $F_{R(LT)}$–$F_{R(HT)}$ phase transition. All the investigated ceramics show a relatively steep decrease of P_r in the vicinity of Curie temperature. The coercive field decreases linearly on heating for all the investigated ceramics with Nb_2O_5 content 0.2–1.5 mol%. This field exceeds the value of measuring field at temperatures from the range 10–60°C for the ceramics with Nb_2O_5 content 1.5 to 0.2 mol%, respectively. These temperatures are lower than these one of the $F_{R(LT)}$–$F_{R(HT)}$ phase transition and corresponding anomalies in the $P_r(T)$ course. The course of the $P_r(T)$ curves was obtained only approximately in the range of lower temperatures (dashed lines). The course of the $P_r(T)$ curves differ markedly in this temperature range, when the measuring field is much higher. More detailed data on the behaviour of P_r vs temperature are shown in our earlier paper[19] for the La-doped ceramics with Zr/Ti ratio 92/8.

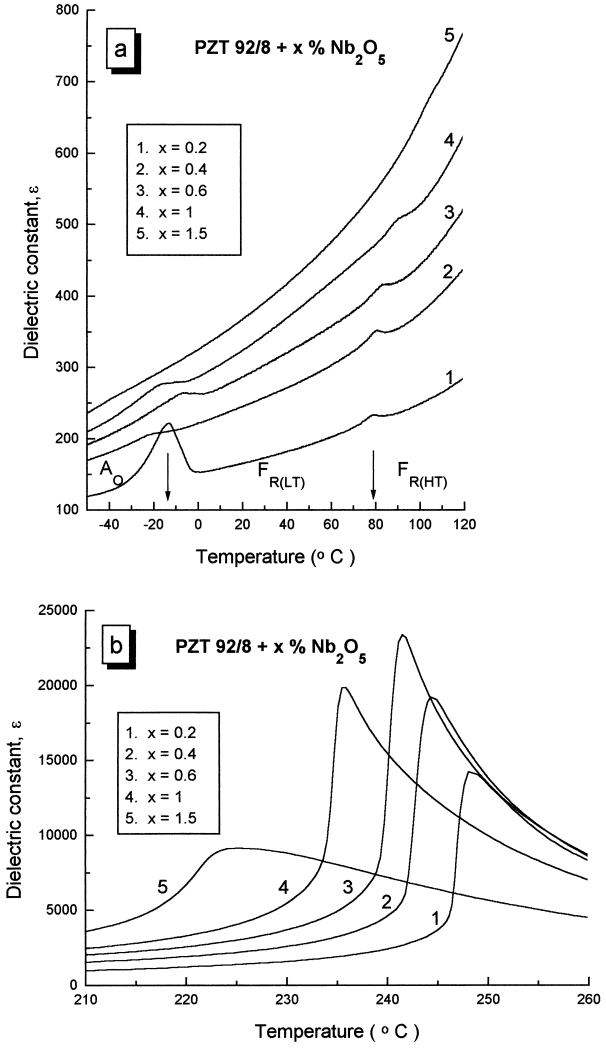

Fig. 4. Dielectric constant vs temperature in the vicinities of the $A_O \rightarrow F_{R(LT)}$ and $F_{R(LT)} \rightarrow F_{R(HT)}$ phase transitions (a) and $F_{R(HT)} \rightarrow P_C$ phase transition (b) for PZT 92/8 + x mol% Nb_2O_5 ceramics.

4. Pyroelectric measurements

In order to determine the pyroelectric coefficient, the ceramic samples were first polarized by DC field of strength 5 kV/cm applied for 10 min at a selected temperature of 300°C and during subsequent cooling to −50°C, under this field. The samples were then heated with a constant rate of 5°C/min through all three phase transitions, starting from the A_O–$F_{R(LT)}$ and ending on the $F_{R(HT)}$–P_C phase transition. The pyroelectric current was recorded numerically as a function of temperature.

The example of pyroelectric current vs temperature for the ceramic with 0.2 mol% Nb_2O_5 is shown in Fig. 8. The recorded current shows pointed peaks at a temperature, which can be identified with the $F_{R(LT)}$–$F_{R(HT)}$ and $F_{R(HT)}$–P_C phase transition temperatures.

The dependence of a pyroelectric coefficient γ vs temperature, obtained for the ceramics with various contents of Nb_2O_5 is shown in Fig. 9. The $\gamma(T)$ curves, shown in the Fig. 9(a) and (b) concerns the $F_{R(LT)}$–$F_{R(HT)}$ and $F_{R(HT)}$–P_C phase transitions, respectively. Both corresponding peaks in the γ(T) curves are strongly dependant on the Nb_2O_5 content and they are relatively sharp when this content does not exceed 1 mol%, whereas they are fairly broad in case of greater content of this additive.

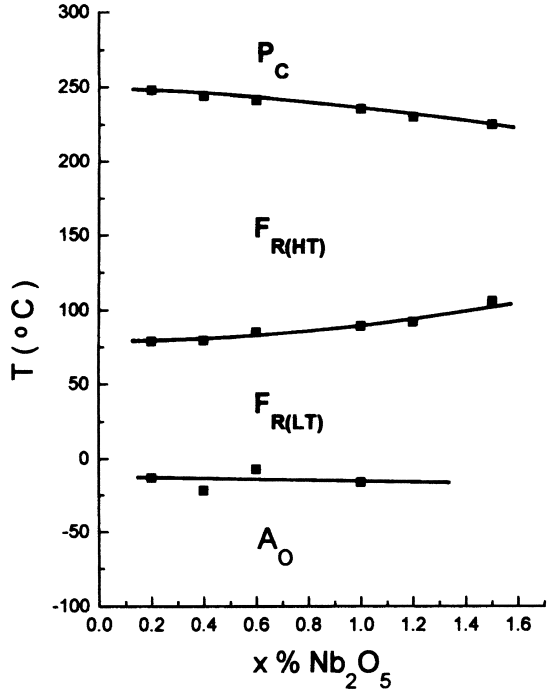

Fig. 5. Variations of phase transition temperatures vs Nb_2O_5 content.

5. The influence of Nb_2O_5 additive on electric conductivity and Seebeck coefficient

To study the influence of the substitution of Nb for the Zr/Ti sublattice on the balance of electron-hole carriers the measurements of electric conductivity and the Seebeck coefficient were carried out at temperatures chosen from the wide range of the paraelectric phase (250–500°C).The results obtained at $T=450$°C are shown as an example in Fig. 10. One can notice that the value of electric conductivity increases or decreases in the ceramics with Nb content smaller or larger than ca. 0.8 mol%.

The thermoelectric studies were carried out at the same temperature range in order to determine the type of the electric conductivity. The experimental technique employed was described in our earlier papers.[22,23] The obtained values of the Seebeck coefficient, as a function of Nb_2O_5 content, are shown in Fig. 10. As may be seen the Seebeck coefficient initially decreases due to the influence of the Nb dopand, whereas for the content larger than ca. 1.2 mol% it increases with increase in Nb_2O_5 content. The near zero values of the Seebeck coefficient for the ceramics with 1–1.2 mol% Nb_2O_5 content indicate a compensated state of electron and hole carriers.

6. Discussion

A review of results obtained confirm the strong influence of the Nb_2O_5 dopant on the $F_{R(LT)}$–$F_{R(HT)}$ and $F_{R(HT)}$–P_C phase transition temperatures. Both dielectric and pyroelectric measurements show an increase of the $F_{R(LT)}$–$F_{R(HT)}$ and a decrease of the $F_{R(HT)}$–P_C phase transition temperatures with an increase in the Nb_2O_5 content. The Nb_2O_5 addition broadens these phase transitions, especially strongly when its content

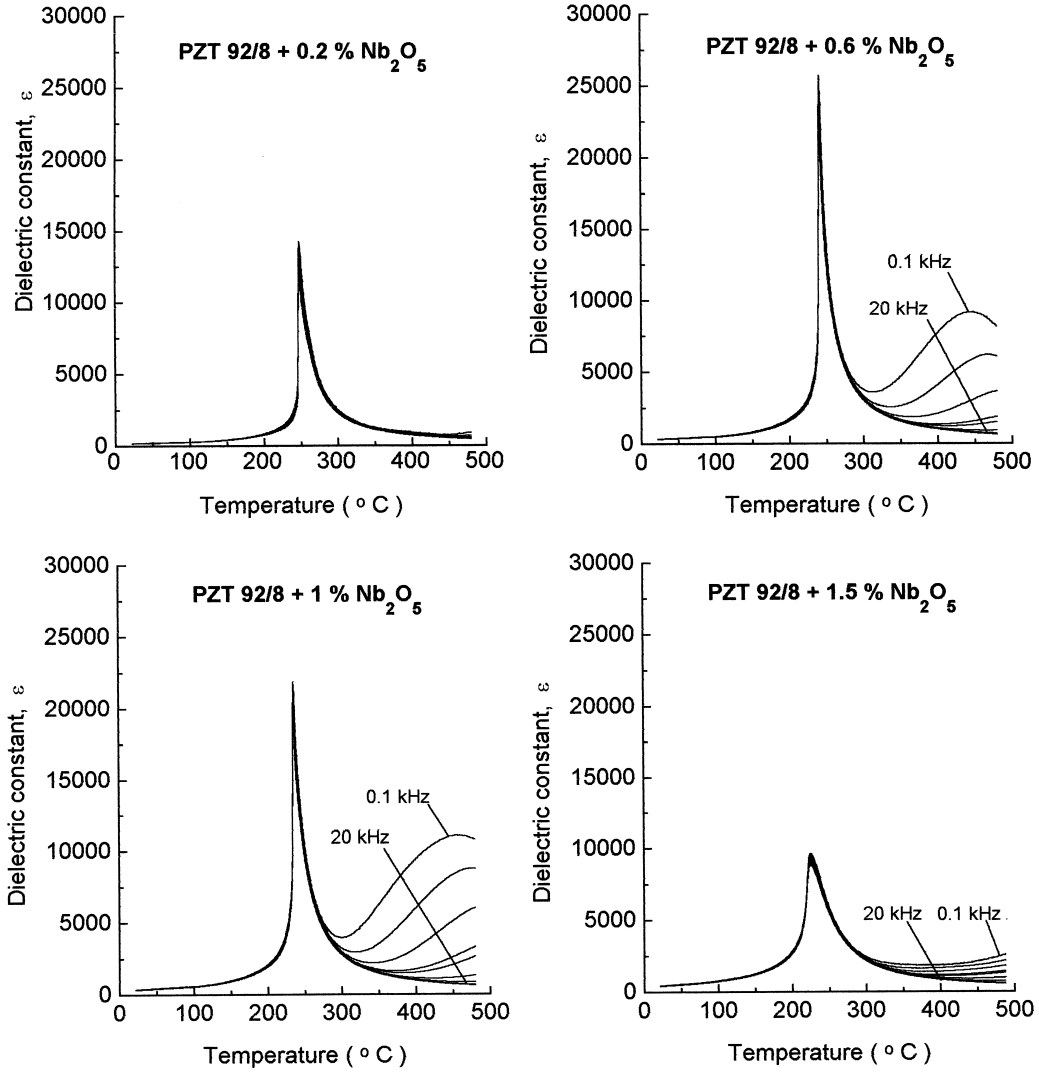

Fig. 6. Dielectric constant as a function of temperature, measured at various frequencies of measuring field, for PZT 92/8 ceramics with shown Nb_2O_5 content. The individual curves from the top to the bottom concern frequencies: 0.1; 0.2; 0.4; 0.8; 1; 2; 4; 10 and 20 kHz.

exceedes ca. 1 mol%. The strongly broadened characteristic of the A_O–$F_{R(LT)}$ phase transition makes it difficult to determine the influence of Nb_2O_5 on this transition. The dependence of the A_O–$F_{R(LT)}$ phase transition temperature vs Nb_2O_5 content (Fig. 5) is only approximate. It is worth noting that Nb_2O_5 dopant content up to about 0.8 mol% results in a considerable improvement of dielectric properties, whereas for its greater content a negative effect is observed (Figs. 4, 6 and 7). It may be interesting to note that electric conductivity and the Seebeck coefficient vs Nb_2O_5 content, behave in a reverse way in these two ranges of concentrations (Fig. 10).

The drastic differentiation in electric and pyroelectric properties of the Nb-doped $Pb(Zr_{0.92}Ti_{0.08})O_3$ ceramics in the above mentioned two ranges in the Nb_2O_5 contents, also relates to their grain structure. The image of the grain structure, shown in Fig. 1 reveals that Nb_2O_5 addition from < 1 mol% produces slightly bigger grains with increase in concentration and it yields a rather uniform grain structure. The ceramics with larger Nb_2O_5 content show a drastically different grain structure, with two kinds of grains: the ones similar to those seen in ceramics with smaller Nb_2O_5 content, and the new one, with grain size one order of magnitude smaller. It seems that the ceramics with Nb_2O_5 content greater than ~ 1 mol% are a mixture of various phases. Our TEM measurements revealed only larger Nb and smaller Zr contents in grains of the smallest dimensions (Figs. 1 and 2). These measurements do not seem sufficient to check if the "nests" of small grains shown in Fig. 1(b) represent grains of $PbNb_2O_6$, as suggested in Ref. 12

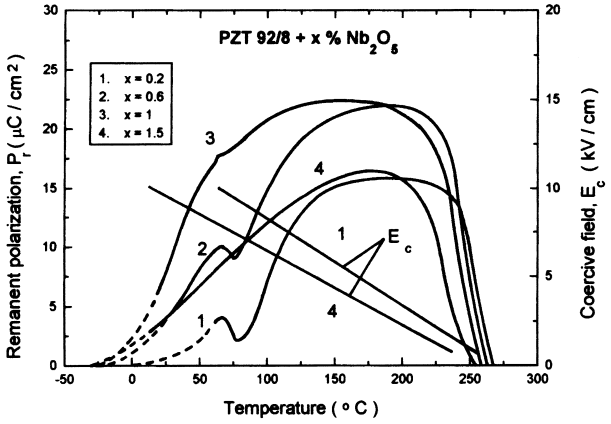

Fig. 7. Remanent polarization and coercive field vs temperature, obtained from hysteresis loop measurements for PZT 92/8 + x mol% Nb_2O_5 ceramics.

The broadened character of all the structural phase transitions also reveals the coexistence of the neighbouring phases of various types of electric order (i.e. AFE, FE and PE) in the vicinities of the phase transitions, in the component $Pb(Zr_{0.92}Ti_{0.08})O_3$ of perovskite structure. This fact was proved by us in our earlier papers by X-ray measurements of the undoped $Pb(Zr_{0.92}Ti_{0.08})O_3$[18,19] and Nb-doped $PbZrO_3$ ceramics.[21] We also proved that for the Nb-doped $PbZrO_3$ ceramics the character of the A_O–F_R and F_R–P_C phase transition broadening is markedly different in the ranges of Nb_2O_5 content smaller and larger than about 1.2 mol%.[21] The A_O–F_R and F_R–P_C phase transitions are very strongly broadened in the range of larger Nb_2O_5 content and all the phases A_O, F_R and P_C coexist in a wide temperature range and the sample is monophase within the P_C phase only at high temperatures. In

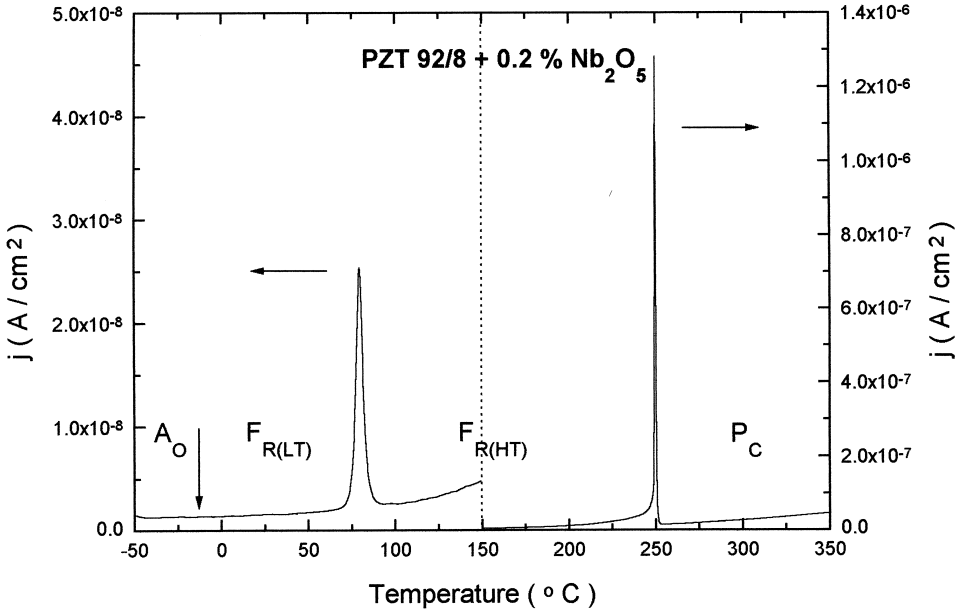

Fig. 8. Changes of pyroelectric current in the vicinities of phase transitions for PZT 92/8 + 0.2 mol% Nb_2O_5.

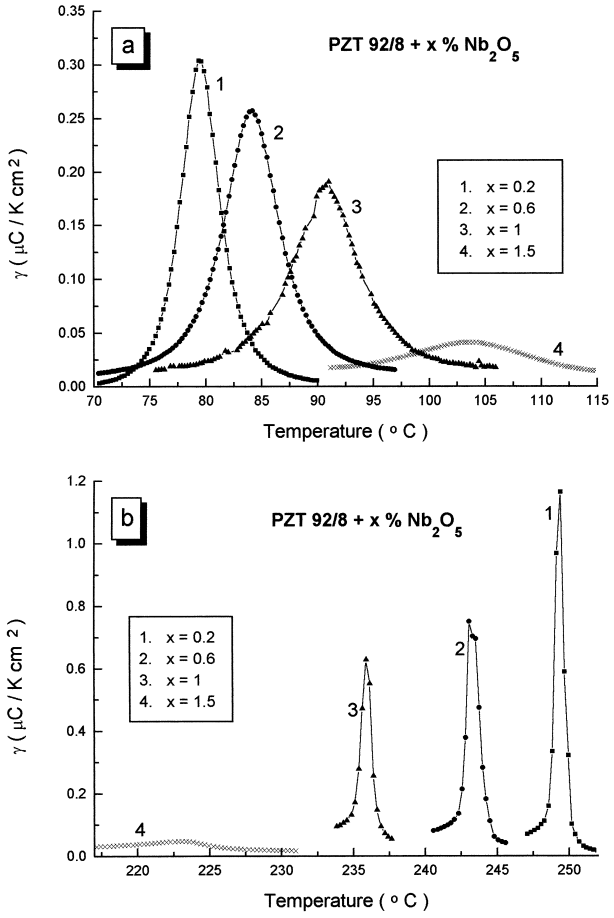

Fig. 9. The pyroelectric coefficient as a function of temperature in the vicinities of the $F_{R(LT)} \rightarrow F_{R(HT)}$ (a) and $F_{R(HT)} \rightarrow P_C$ (b) phase transitions for PZT $92/8 + x$ mol% Nb_2O_5 ceramics.

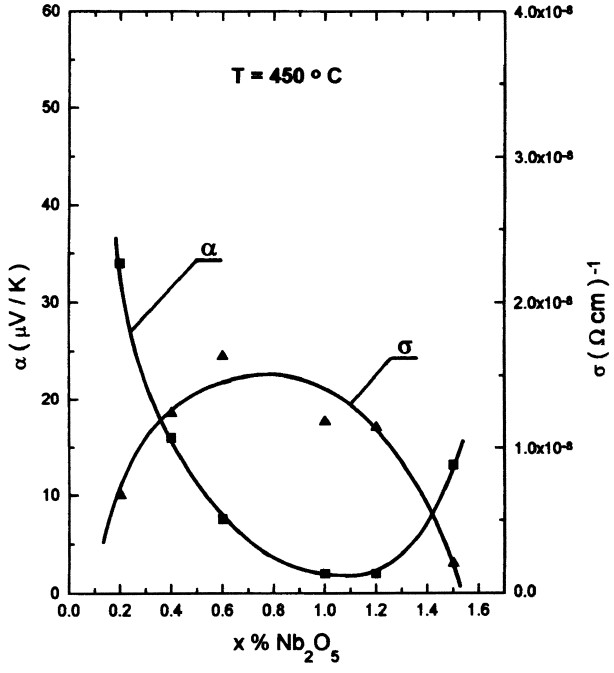

Fig. 10. The Seebeck coefficient (α) and electric conductivity (σ), obtained at $T = 450°C$, vs Nb_2O_5 content.

contrast to this case the phase transitions are distinctly determinable and the F_R phase contents reaches 100% at a certain temperature range in the case of smaller Nb_2O_5 content.

It has already been shown that the substitution of Nb^{5+} ions for Zr^{4+}/Ti^{4+} ions is the most likely phenomena.[7,12,21] This process should be accompanied by the effect of an increase of Pb-position vacancy concentration. Additional vacancies in the Pb and O sublattices are caused by PbO sublimation. The presence of Pb and O vacancies exerts a strong influence on the balance of charge carriers transport process. As it is known from earlier studies[21–23] the $PbZrO_3$ and Zr-rich PZT ceramics exhibit electric conductivity of p-type caused by predomination of Pb-vacancies which act as acceptor centres. Analysis of the electric conductivity and the Seebeck coefficient studies (Fig. 10) leads to the conclusion that for low Nb-doped samples, i.e. when $Nb_2O_5 < 1$ mol%, the Nb^{5+} ions substituted for Zr^{4+}/Ti^{4+} play the role of donors. Initially this leads to an increase of conductivity due to increase in concentration of electron carriers and decrease of the positive Seebeck coefficient owing to the compensation of already existing holes by electrons, originating from the donor dopant.

The fact of the nearly full compensation of p-type conductivity with the 1 mol% of Nb_2O_5-dopant acting as donor (Fig. 10), occurs, proves that there exists a relatively low concentration of Pb-vacancies, acting as acceptors. Probably this is due to the technological conditions which reduce the PbO sublimation during sintering.

When Nb_2O_5 content exceeds 0.8–1 mol% a further change of electroconductivity and Seebeck coefficient is observed, but then σ decreases and α increases (Fig. 10). Also drastic changes in dielectric and pyroelectric properties are observed in these samples (Figs. 4, 6, 7 and 9). Maybe they represent a mixture of the main compound of perovskite structure $Pb(Zr,Ti)O_3$ and $PbNb_2O_6$ of different structure. As mentioned above the regions with various types of electric ordering (A_O, $F_{R(LT)}$, $F_{R(HT)}$ and P_C) occur also in a wide temperature range. These two kinds of heterogeneity, and the more complex grain structure (Fig. 1), are likely to be responsible for the observed changes in the electric (ε, P_r, σ), thermoelectric (α) and pyroelectric (γ) properties and their temperature characteristics.

References

1. Jaffe, B., Cook, W. R. and Jaffe, H., *Piezoelectric Ceramics*. Academic Press, London and New York, 1971.
2. Haertling, G. H., PLZT elektrooptic materials and applications — a review. *Ferroelectrics*, 1987, **75**, 25.
3. Buchanan, R.C., *Ceramic Materials for Electronics*. Chapter 3: G.H.Haertling, New York, 1991.

4. Wentz, I. L. and Kennedy, L. Z., Primary pyroelectric effect in the PZT-95/5 ceramics. *J. Appl. Phys*., 1964, **35**, 1767.
5. Clarke, R. and Whatmore, R. W., The growth and characterization of $PbZr_xTi_{1-x}O_3$ single crystals. *J. Cryst. Growth*, 1976, **33**, 525.
6. Fritz, I. J. and Keck, I. D., Pressure-temperature phase diagrams for several modified lead zirconate ceramics. *J. Chem. Solids*, 1978, **39**, 1163.
7. Hardiman, B., Kiehl, K. V., Reeves, C. P. and Zeyfang, R. R., Lead titanate zirconate-based pyroelectric ceramics. *Ceramurgia International*, 1978, **4**(3), 108.
8. Glazer, A. M. and Mabud, S. A., Powder profile refinement of lead zirconate titanate at several temperatures. *Acta Cryst*., 1978, **B34**, 1060.
9. Dai, X. and Wang, Y., Multistage heat-electric energy convertion working on $F_{R(LT)}$–$F_{R(HT)}$ phase transition in Nb-doped PZT-97/3 ceramics. *Ferroelectrics*, 1990, **109**, 253.
10. Wang, Y.L. and Lin, S.W., Research in inorganic materials. Acad. Sci., 1980, 154.
11. Chang, Y., A TEM study of crystal and domain structures of Nb-doped 95/5 PZT ceramics. *J. Appl. Phys*., 1982, **29**, 237.
12. Duan, N., Cereceda, N., Noheda, B. and Gonzalo, J. A., Dielectric characterization of the phase transitions in $Pb_{1-y/2}(Zr_{1-x}Ti_x)_{1-y}Nb_yO_3$ ($0.03 \leqslant x \leqslant 0.04$, $0.02 \leqslant y \leqslant 0.05$). *J. Appl. Phys*., 1996, **82**(2), 779.
13. Dai, X. W., Li, J. F. and Viehland, D., Constriction of the polarization by incoherent oxygen octahedral tilting in rhombohedral-structured lead zirconate titanate. *J. Appl. Phys*., 1995, **77**(7), 3354.
14. Gundel, H., Riege, H., Wilson, E. J. N., Hańderek, J. and Zioutos, K., Copious electron emission from PLZT ceramics with a high zirconium concentration. *Ferroelectrics*, 1989, **100**, 1.
15. Gonzalo, J. A., Wang, Y. L., Noheda, B., Lifante, G. and Koralewski, M., Direct conversion of thermal energy to electric energy by means of ferroelectrics materials. *Ferroelectrics*, 1995, **153**, 347.
16. Hańderek, J., Ujma, Z., Carabatos-Nedelec, C., Kugel, G. E., Dmytrów, D. and El-Harrad, I., Dielectric, pyroelectric, and thermally stimulated depolarization current investigations on lead-lanthanum zirconate-titanate x/95/5 ceramics with La content $x = 0.5\%$–4%. *J. Appl. Phys*., 1993, **73**, 367.
17. Ujma, Z., Hańderek, J. and Kugel, G. E., Phase transitions in Nb-doped $Pb(Zr_{0.95}Ti_{0.05})O_3$ ceramics investigated by dielectric, pyroelectric and Raman scattering measurements. *Ferroelectrics*, 1997, **198**, 77.
18. Ujma, Z., Hańderek, J., Pawełczyk, M., Hassan, H., Kugel, G. E. and Carabatos-Nedelec, C., The antiferroelectric-ferroelectric-paraelectric phase sequence in lead-lanthanum zirconate-titanate ceramics with 8% Ti content. *J. Phys.: Condens. Matter*, 1994, **6**, 6843.
19. Ujma, Z., Hańderek, J., Hassan, H., Kugel, G. E. and Pawełczyk, M., Phase transitions in lead-lanthanum zirconate-titanate ceramics with a Zr/Ti ratio of 92/8 and La content of up to 1 at%. *J. Phys.: Condens. Matter*, 1995, **7**(5), 895.
20. Benguigui, L., Ferroelectricity and antiferroelectricity in pure and Nb_2O_5doped lead zirconate. *J. Solid State Chem*., 1971, **3**, 381.
21. Ujma, Z., Dmytrów, D. and Pawełczyk, M., Structure and electrical properties of $PbZrO_3$. *Ferroelectrics*, 1991, **120**, 211.
22. Hańderek, J., Wróbel, Z., Wójcik, K. and Ujma, Z., Specific problems of thermoelectric force investigations in lead titanate, potassium niobate, and sodium niobate single crystals and in lead zirconate ceramics. *Ferroelectrics*, 1977, **17**, 60.
23. Ujma, Z. and Hańderek, J., Phase transitions and spontaneous polarization in $PbZrO_3$. *Phys. Stat. Sol. (a)*, 1975, **28**, 489.